COMPARATIVE THREE-DIMENSIONAL FLOW ANALYSIS OF MHD GENERATORS AND SEAWATER THRUSTERS

Ezzat D. Doss

Argonne National Laboratory
Argonne, Illinois 60439, U.S.A.

and

Gabriel D. Roy
Office of Naval Research
Arlington, Virginia 22217, U.S.A

28th Symposium

Engineering Aspects of Magnetohydrodynamics

June 26-28, 1990

Chicago, Illinois

COMPARATIVE THREE-DIMENSIONAL FLOW ANALYSIS OF MHD GENERATORS AND SEAWATER THRUSTERS

Ezzat D. Doss
Engineering Physics Division
Argonne National Laboratory, Argonne, Illinois 60439

Gabriel D. Roy
Mechanics Division
Office of Naval Research, Arlington, Virginia 22217

ABSTRACT

The three-dimensional flow characteristics inside MHD plasma generators and seawater thrusters are analyzed by solving the governing partial differential equations for flow and electrical fields. The equation set consists of the mass continuity equation, the three momentum equations, the equations for enthalpy, turbulence kinetic energy and its dissipation rate, and the Maxwell equations.

Calculations have been performed for a Faraday plasma generator and for a continuous electrode seawater thruster. The numerical results of those two applications are compared. Calculations have been made to study the flow evolution in MHD generators and thrusters. The calculations show that velocity overshoots friction enhancement exist over the sidewalls and are strongly manifested in MHD generators but not so in MHD thrusters. Plots of velocity and skin friction are presented to illustrate the flow development in MHD generators and thrusters.

INTRODUCTION

Extensive work has been done on channel flow inside open-cycle MHD plasma generators,[1-7] but there has been minimal research effort on duct flow inside MHD seawater thrusters. However, MHD flow inside those ducts is subject to J x B forces whether the duct is an MHD generator or an accelerator. In the first case, for generators, electrical power is extracted from the interaction of the fluid flow with the magnetic field. In the accelerator case, energy is supplied to the duct by applying an external electrical field, and the resulting electrical currents interact with the magnetic field to produce a driving force that pushes the fluid through the duct. This is the case of an MHD thruster. There are obviously some differences between the flow medium and the operating condictions between the two applications; however, the governing equations and the physical phenomena are quite similar.

For the purpose of analyzing the performance of MHD generators or thrusters, there are three possible orders of conducting the analysis. In the first, namely, one-dimensional analysis, the cross-stream variations are neglected and only the axial development of velocity, temperature, etc., are calculated. There is a sizable body of literature about such analyses for MHD generators,[8] and to a much lesser extend for MHD thrusters.[9-14] Although the one-dimensional models are computationally fast, they are inherently less accurate than the multi-dimensional models. An improvement over the one-dimensional analyses are two-dimensional analyses, such as those reported by Doss, et al.[4] In these, it is assumed that the important directions of variation are the electrode and the flow directions. Therefore, the profiles of variables in the sidewall direction are assumed to be uniform. Development of flow asymmetries between the anode and cathode walls due to the presence of Hall current are discussed. Applications of this model for performance analysis and design of large-scale MHD channels are presented in Ref. [5].

Quasi-three-dimensional models and the fully-developed cross plane solutions provide further improvements over the two-dimenional analyses. Ahluwalia and Doss[6] developed a quasi-three-dimensional analysis procedure that accounts for the effects of the sidewall boundary layers. This analysis prescribes the boundary layer parameters on the sidewalls, and accounts for the area reduction resulting from the sidewall boundary layer growth. The procedure is not, however, designed to predict secondary flows and velocity overshoots. Using a simplified quasi-three-dimensional approach, in which the two-dimensional solution of the flow between the electrode walls is allowed to interact with the flow over the sidewalls, the development of velocity overshoots on the sidewalls of the MHD generators has been explained.[1]

On the experimental side, Roy and Wu[7] performed a comparison study between the analytical results and experimental data for the pressure distribution along supersonic generator channel.

In summary, the literature on MHD channel flow for plasma open-cycle generators indicate that the flow and electrical fields in MHD generators are inherently three-dimensional for a variety of reasons. The interaction of the MHD electrical forces (JxB) with the fluid flow leads to flow distortions.[2,3] The cross-sectional nonuniformity of the axial component of the Lorentz force (J_yB) is directly responsible for the generation of velocity overshoots in the boundary layers. The nonuniformity in the magnetic field direction of the Lorentz force due to Hall current (J_xB) produces secondary flows which in turn lead to flow asymmetry.

For MHD seawater thrusters, however, the electrical conductivity of seawater is expected to be practically uniform across and along the thruster provided the effect of bubbles formation, due to electrolysis, on the electrical conductivity is minimum. The Hall parameter for seawater thruster is also negligible. Therefore one might anticipate that such flow nonuniformities would not be manifested strongly inside the ducts as much as is the case of plasma generators. In order to investigate the extent of such flow nonuniformities in the thrusters, three-dimensional calculations of the flow and electrical fields have to be performed.

The purpose of the present paper is to describe a three-dimensional model that have been developed and applied to analyze the development of the flow fileds inside MHD generators and seawater thrusters.

GASDYNAMIC MODEL

Governing Equations

The flow processes in the MHD channel are represented by the three-dimensional Navier-Stokes equations. However, because this flow is predominantly along the axial direction, certain simplifications can be made by consideration of the order of magnitude of various terms. The simplification made here is referred

to as the parabolic approximation, which consists of: a) neglecting the diffusional fluxes in the axial direction and b) considering the pressure gradient in the axial momentum equation to be uniform over the duct cross section. The parabolic approximation does not introduce any significant errors when the flow is predominantly one-way, but it makes the calculation procedure very economical from the computational viewpoint.

Mean Flow Equations

Mass Continuity $\frac{\partial}{\partial x}(\rho u) + \frac{\partial}{\partial y}(\rho v) + \frac{\partial}{\partial z}(\rho w) = 0$

x-momentum $\frac{\partial}{\partial x}(\rho uu) + \frac{\partial}{\partial y}(\rho vu) + \frac{\partial}{\partial z}(\rho wu) = -\frac{\partial \bar{p}}{\partial x} + \frac{\partial \tau_{xy}}{\partial y} + \frac{\partial \tau_{xz}}{\partial z} + J_y B$

y-momentum $\frac{\partial}{\partial x}(\rho uv) + \frac{\partial}{\partial y}(\rho vv) + \frac{\partial}{\partial z}(\rho wv) = -\frac{\partial p}{\partial y} + \frac{\partial \tau_{yy}}{\partial y} + \frac{\partial \tau_{yz}}{\partial z} - J_x B$

z-momentum

$$\frac{\partial}{\partial x}(\rho uw) + \frac{\partial}{\partial y}(\rho vw) + \frac{\partial}{\partial z}(\rho ww) = -\frac{\partial p}{\partial z} + \frac{\partial \tau_{zy}}{\partial y} + \frac{\partial \tau_{zz}}{\partial z}$$

Enthalpy $\frac{\partial}{\partial x}(\rho uh) + \frac{\partial}{\partial y}(\rho vh) + \frac{\partial}{\partial z}(\rho wh) = -\frac{\partial q_y}{\partial y} - \frac{\partial q_z}{\partial z} + u\frac{\partial \bar{p}}{\partial x} + v\frac{\partial p}{\partial y} + w\frac{\partial p}{\partial z} + \frac{J^2}{\sigma} + D$

where

$$D = (\mu_\ell + \mu_t)\left[2\left\{\left(\frac{\partial w}{\partial z}\right)^2 + \left(\frac{\partial v}{\partial y}\right)^2\right\} + \left(\frac{\partial w}{\partial y} + \frac{\partial v}{\partial z}\right)^2 + \left(\frac{\partial u}{\partial z}\right)^2 + \left(\frac{\partial u}{\partial y}\right)^2\right]$$

State Equation

$$\rho = \rho(\bar{p}, h),$$

For seawater applications, ρ is assumed to be constant; its value depends on the physical location and temperature of the seawater.

Turbulence Model

The turbulent fluxes are represented as the product of a turbulent viscosity and the gradients of the flow variable. The turbulent viscosity is calculated from the local values of the turbulent kinetic energy (k) and its dissipation rate (ε), from the formula

$$\mu_t = C_\mu \rho K^2/\varepsilon$$

The turbulent fluxes are calculated by the following formulae.

$$\tau_{ij} = (\mu_t + \mu_\ell)\left(\frac{\partial u_i}{\partial x_j} + \frac{\partial u_j}{\partial x_i}\right), \quad q_i = -\left(\frac{\mu_t}{\sigma_h} + \frac{\mu_\ell}{\sigma_\ell}\right)\left(\frac{\partial h}{\partial x_i}\right)$$

The values of k and ε are obtained from the solution of following transport equations.

Kinetic Energy of Turbulence

$$\frac{\partial}{\partial x}(\rho uk) + \frac{\partial}{\partial y}(\rho vk) + \frac{\partial}{\partial z}(\rho wk) = \frac{\partial}{\partial y}\left(\frac{\mu_t}{\sigma_k}\frac{\partial k}{\partial y}\right) + \frac{\partial}{\partial z}\left(\frac{\mu_t}{\sigma_k}\frac{\partial k}{\partial z}\right) + G - \rho\varepsilon$$

Dissipation Rate

$$\frac{\partial}{\partial x}(\rho u\varepsilon) + \frac{\partial}{\partial y}(\rho v\varepsilon) + \frac{\partial}{\partial z}(\rho w\varepsilon) = \frac{\partial}{\partial y}\left(\frac{\mu_t}{\sigma_\varepsilon}\frac{\partial \varepsilon}{\partial y}\right) + \frac{\partial}{\partial z}\left(\frac{\mu_t}{\sigma_\varepsilon}\frac{\partial \varepsilon}{\partial z}\right) + \frac{C_1 G\varepsilon}{k} - C_2\rho\frac{\varepsilon^2}{k}$$

Where G represents the production of the kinetic-energy of turbulence as a result of the interaction of the shear stresses and the velocity gradients.

The expression for G after the neglect of axial gradients is as follows,

$$G = \mu_t\left[2\left\{\left(\frac{\partial v}{\partial y}\right)^2 + \left(\frac{\partial w}{\partial z}\right)^2\right\} + \left(\frac{\partial u}{\partial y}\right)^2 + \left(\frac{\partial u}{\partial z}\right)^2 + \left(\frac{\partial v}{\partial z} + \frac{\partial w}{\partial y}\right)^2\right]$$

Near Wall Representation

In turbulent flows, the gradients of flow variables adjacent to solid walls are very steep, and in order to resolve these gradients a very fine finite-difference mesh is required. Not only is such an approach expensive, but the present turbulence model, which is designed for high Reynolds numbers, is invalid in regions very close to the wall. The present model, therefore, uses what is known as the wall function approach which is described in Refs.[3,15]

Solution Procedure

The procedure used to solve the partial-differential equations employs a marching scheme in which the solution to the differential equations is obtained at successive cross-sectional planes from the inlet to the exit of the duct. Because it was assumed that the flow is predominantly one-way, the influences travel always along the flow direction and, therefore, the flow properties at a given axial station can be calculated solely from their values at the previous station. This eliminates the need to iterate back and forth between the inlet and the exit of the channel.

At each axial station, the equations for u, v, w, h, k, ε, and the electric potential are solved in their finite-difference form. The pressure fields, are obtained from the satisfaction of the continuity equation. The details of the finite-differencing are given in Refs.[3,15]. One main consequence of the marching algorithm is that all the flow variables are stored only as two-dimensional arrays. This significantly reduces the required computer storage and CPU time.

ELECTRICAL MODEL

Governing Equations

Under the MHD approximations, the electric field, E, and the current density, J, are governed by the following Maxwell equations and Ohms law.

$$\nabla \times \vec{E} = 0, \quad \nabla \cdot \vec{J} = 0, \quad \vec{J} = \sigma(\vec{E} + \vec{U} \times \vec{B}) - \frac{\beta}{B}\vec{J} \times \vec{B}$$

Because of the form of Maxwell equations, it is possible to define an electric potential, ψ, such that

$$\vec{E} = -\nabla\psi$$

It is assumed that the magnetic field, B, is sectionally uniform and is oriented along the z-direction.

A difficulty in performing complete three-dimensional flow and electrical analyses of MHD generators is that the calculation of electric fields in a finitely, segmented channel is an extremely slow process. One way to alleviate this difficulty, is to use the infinite segmentation approximation in which, the electrical fields are assumed to vary slowly in the flow direction in comparison to their variations in the cross-flow direction. Such an assumption is made in the present study. A consequence of the assumed slow axial variations is that E_x is a constant, allowing ψ to be represented in the form $\psi = -x.E_x + \phi(y,z)$,

In the above, E_x is to be determined subsequently from the specification of the external connection. On substituting the following equation for the two-dimensional function, $\phi(y,z)$, results:

$$\frac{\partial}{\partial y}\left(\sigma_n \frac{\partial \phi}{\partial y}\right) + \frac{\partial}{\partial z}\left(\sigma \frac{\partial \phi}{\partial z}\right) = E_x \frac{\partial}{\partial y}\left[(\beta - \cot\gamma)\sigma_n\right]$$

$$- \frac{\partial}{\partial y}\left[\sigma_n B (u - \beta v)\right]$$

where $\sigma_n = \sigma/(1+\beta^2)$, and γ is 90 degrees for the Faraday connection.

Solution Procedure

The last equation, subject to the appropriate boundary conditions for the Faraday generator $\langle J_x \rangle = 0$, and for continuous electrode thruster ($E_x = 0$) form a two-dimensional elliptic problem.

It is solved numerically by a finite-difference method. In order to account for rapid variations in the flow and electrical variables near the channel walls, a finer mesh is employed in the near-wall region than in the core. The finite-difference equations are solved by the tridiagonal matrix algorithm used for the gasdynamic equations. The convergence of the solution is rapid.

APPLICATIONS AND RESULTS

Operating Conditions

Computations have been performed using the three-dimensional model described before for an MHD plasma generator operating in the Faraday mode with insulating sidewalls and for an MHD thruster operating in the continuous electrode mode with insulating sidewalls. The general operating parameters for the applications considered are listed in Table I. The flow at the entrance of the generator and thruster is assumed to be that of a plug flow.

Flow Fields and Friction Factor

A Parametric study has been performed by varying the average electric load factor ($K \equiv \langle E_y \rangle / \langle uB \rangle$) between 0.0 and 0.95 ($K<1.0$) for the MHD generator and between 1 and 20 ($K>1.0$) for the thruster. Sample results are presented and discussed in this paper. Those results are for an MHD generator operating with $K = 0.75$ and for an MHD thruster operating with $K = 2$. More details can be found in Refs.[3,17]

Figures 1 and 2 show surface plots for the calculated axial velocity distributions at several cross-sections along the MHD generator and thruster respectively. The three-dimensional effects caused by the interaction of the Lorentz forces (JxB) with the fluid flow are strongly manifested in the case of the MHD generator as compared to the flow development in the thruster. The axial component of the (J_yB) acts as a retarding force for the generator, while it acts as an accelerating force for the thruster. The J_yB force, however, exists for both cases, and is not uniform over the cross-section. As a result, velocity distortions exists and they are manifested strongly as velocity overshoots in the boundary layer for the MHD generator case. On the other hand the perpendicular component JxB produces cross stream transverse velocities leading to flow asymmetries. For MHD seawater thrusters, operating in the continuous electrode mode and with a negligible Hall parameter, the JxB component is practically non-existent. Therefore, as shown in Figure 2, the flow structure for the thruster case is less complex than that for the generator case.

Table I

Operating Condition for the Illustrated Examples

	Generator	Thruster	
Geometry:			
• length	10	10	m (rectangular)
• height, width (inlet)	0.5 x 0.5	1.0 x 1.0	m^2
• height, width (outlet)	1.0 x 1.0	1.0 x 1.0	m^2
• wall roughness	2.5	2.5	mm
Wall temperature	1800	300	K
Inlet fluid temperature	2760	300	K
Working fluid	Products of combustion of natural gas seeded with potassium	Seawater	
• electrical conductivity	7.2 - 5.1	4.8 (constant)	S/m
Inlet flow velocity	770	30	m/s
Mass flow rate	75	30750	Kg/s
Magnetic field	6	20	T
Duct loading	Faraday with insulating sidewalls	continuous electrode with insulating sidewalls	
• average electric load factor	0.2 - 0.95	1-20	

The physical properties of seawater are documented in Ref. [15] and the values used are for a temperature of 20°C, while those for plasma are obtained from the NASA-Lewis Chemical equilibrium code.

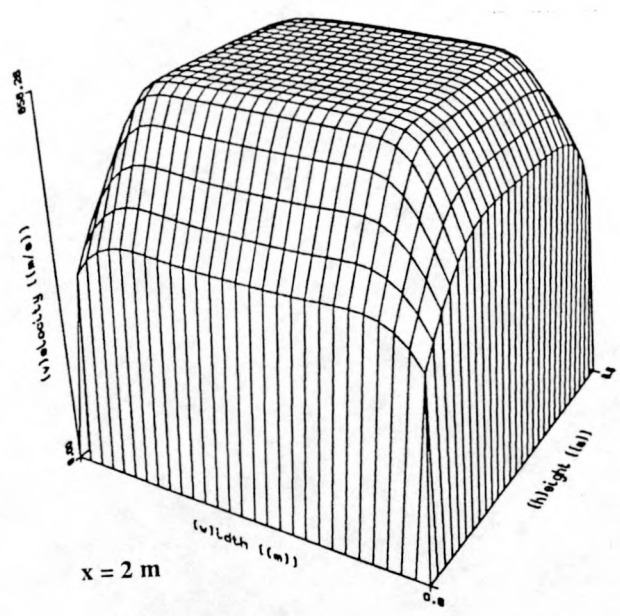

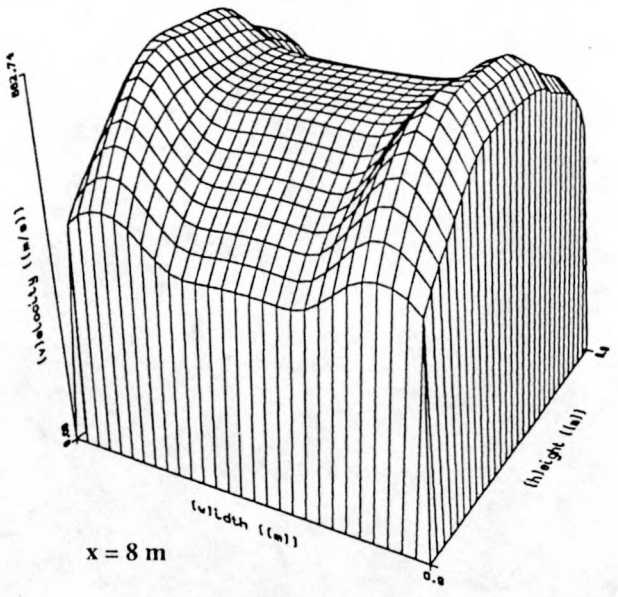

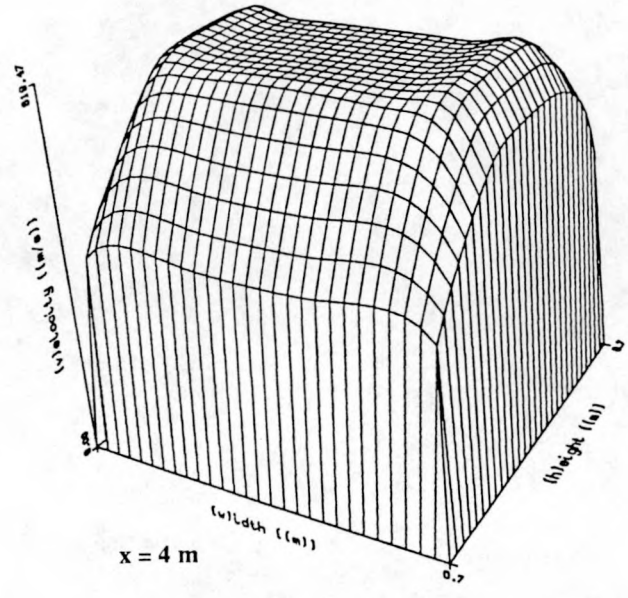

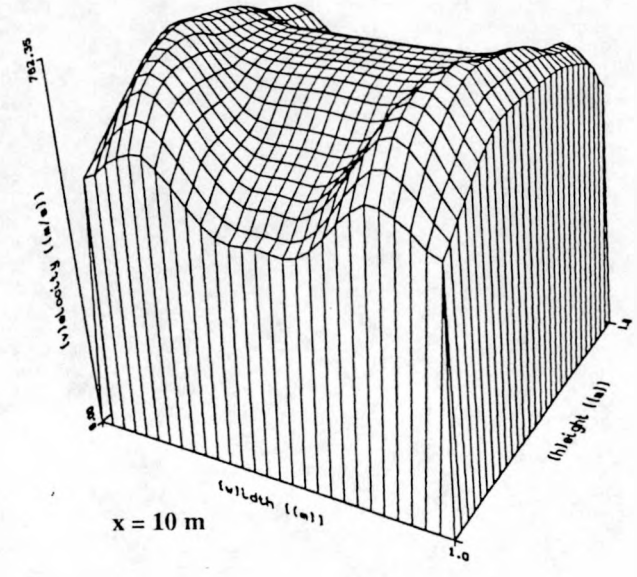

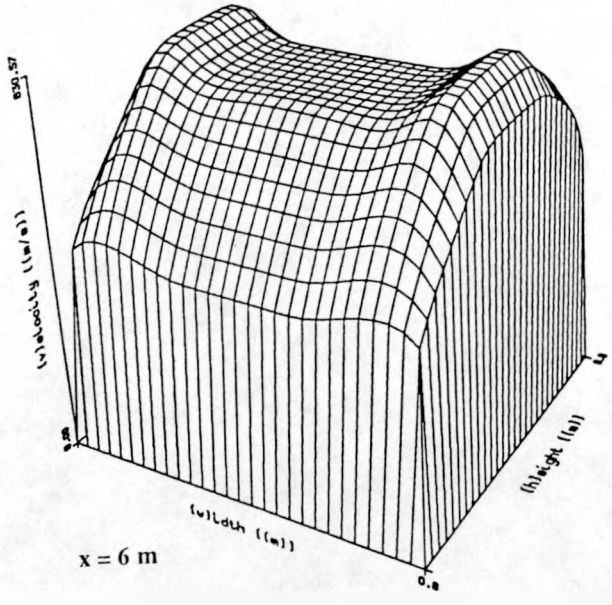

Figure 1. Emergence of velocity overshoots in the sidewall boundary layers on MHD generator (B = 6 T, K = 0.75)

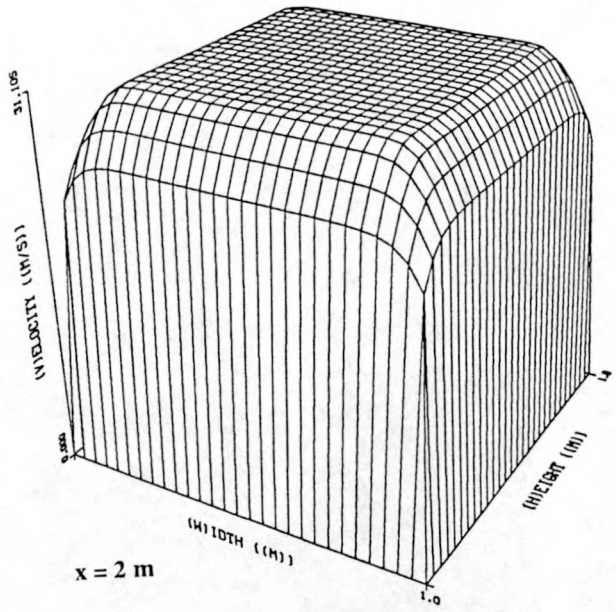

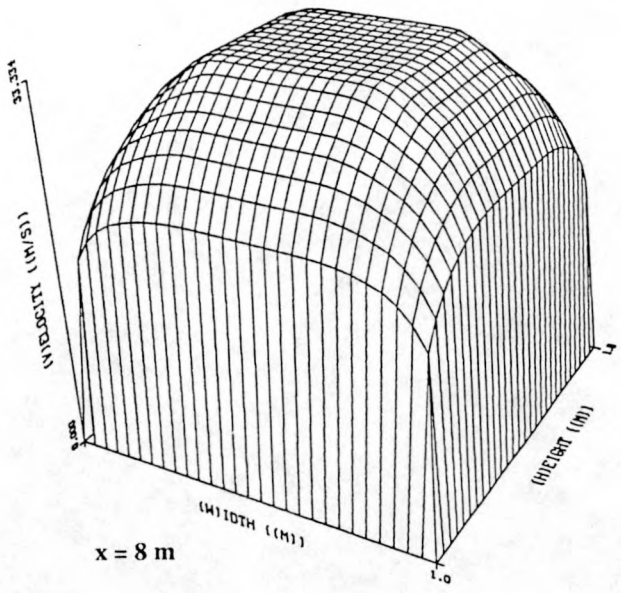

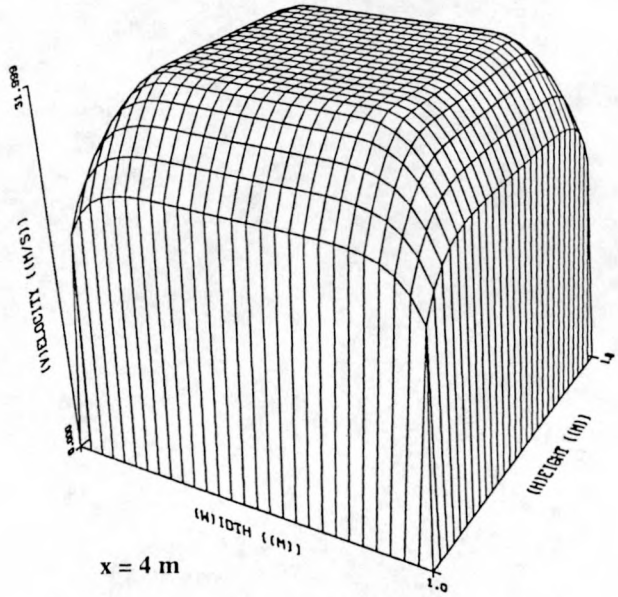

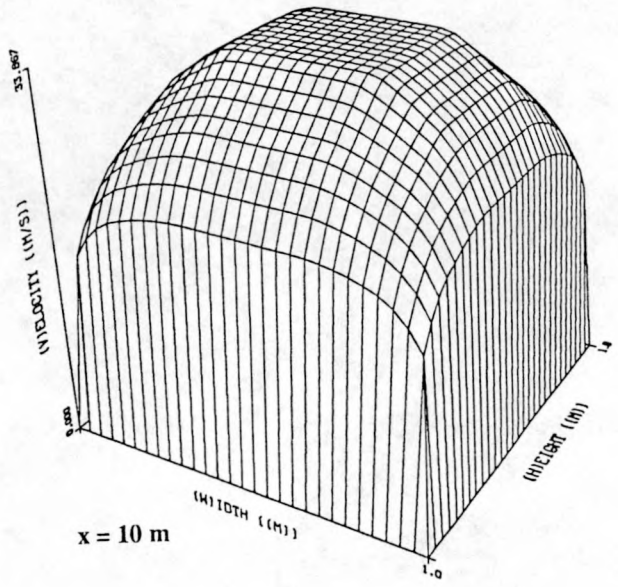

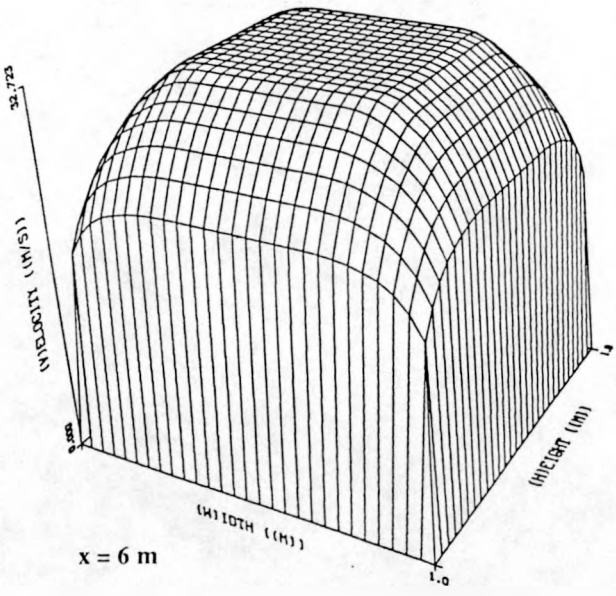

Figure 2. Flow development in MHD thruster
(B = 20T, U = 30 m/s, K = 2)

Figures 3 and 4 present the corresponding axial velocity profiles in the boundary layer for the two applications. At first, one may think that the surface plots for the thruster (Fig. 2) are typical for normal non-MHD turbulent flow. However, Figure 4 indicates that there is a difference between the shape of the axial velocity profile along the electrode wall and that along the sidewall. The velocity near the insulating wall (Hartmann boundary layers) is relatively higher than that near the electrode walls. For the generator case the disparity between the velocity profiles over the two walls is much larger where there is a distinct velocity overshoot in the boundary layers.

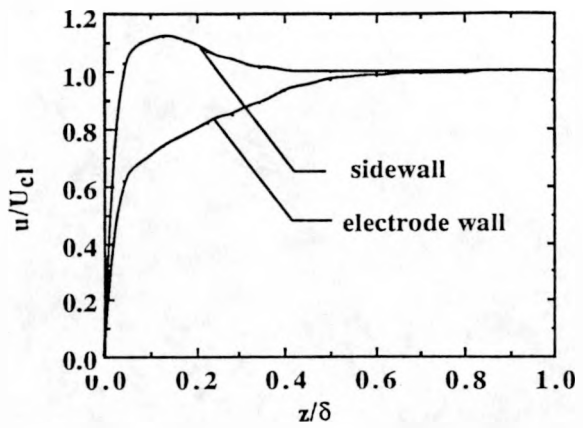

Figure 3. Normalized velocity profiles along the MHD generator (x=8 m)

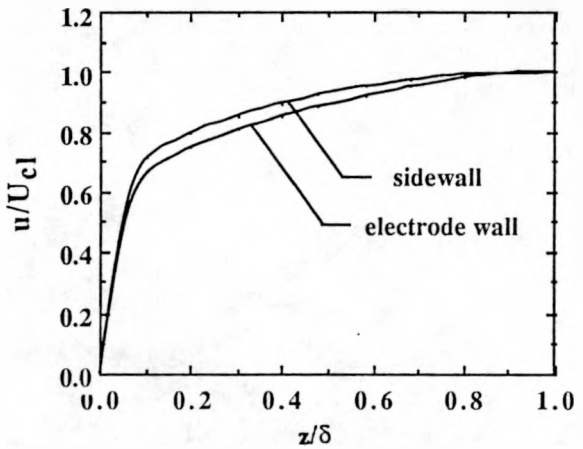

Figure 4. Normalized velocity profiles along thruster walls (x=8 m)

Figures 5 and 6 present the corresponding variation of the J_y component across the duct between the insulating walls for the generator and thruster respectively. The nonuniform J_y distribution acts on the flow differently. For the case of the generator, where the electrical conductivity is very small in the cold boundary layer, J_y is correspondingly very small compared to the core flow values. Accordingly, the retarding J_yB force exerts a less force on the sidewall (Hartmann) boundary layer. In a relative sense, the sidewall boundary layers are accelerated in relation to the central region. This relative acceleration of the sidewall boundary layers results in the observed velocity overshoots.

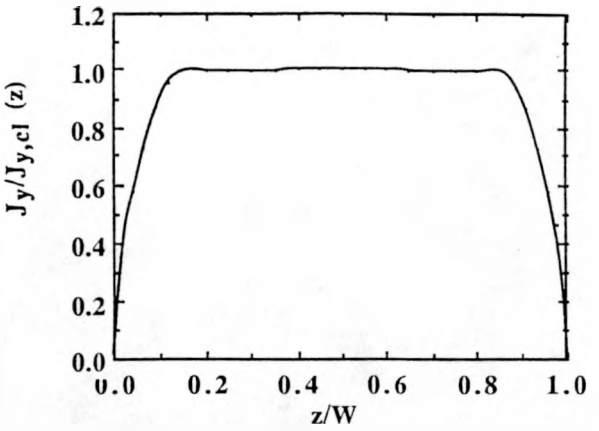

Figure 5. Normalized current density across the sidewalls of the MHD generator (x=8 m)

On the other hand for the MHD thruster case, the seawater electrical conductivity is practically constant (neglecting the effects of bubble formation). Therefore, any change in the sidewall (Hartmann) boundary layers will be caused by the nonuniformity of the velocity profile. For constant electrical potential over the cathode and the anode, the current density is larger in the sidewall boundary layers because of the smaller velocities. Therefore, a larger accelerating force (J_yB) will be felt on the flow in the sidewall boundary layers as compared to the main flow because of the increase of the current density component J_y as shown in Figure 6. Consequently, the velocity profile is flatter over the sidewall in comparison to the velocity profile in the boundary layers over the electrode wall (Fig. 4).

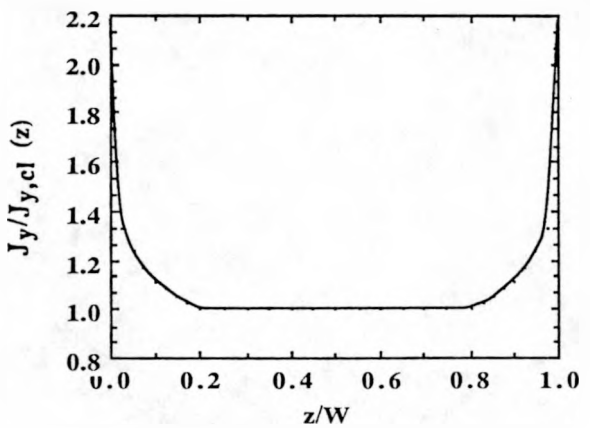

Figure 6. Normalized current density across the sidewalls of the MHD thruster (x=8m)

As a result of such nonuniformities in the flow fields, nonuniform distribution of the skin friction is expected along the duct walls. Figures 7 and 8 present the variation of the friction factor (C_f) along the electrode wall and the sidewall of the MHD generator and thruster respectively. The skin friction is higher on the sidewall for both applications but with a distinct difference for the generator case.

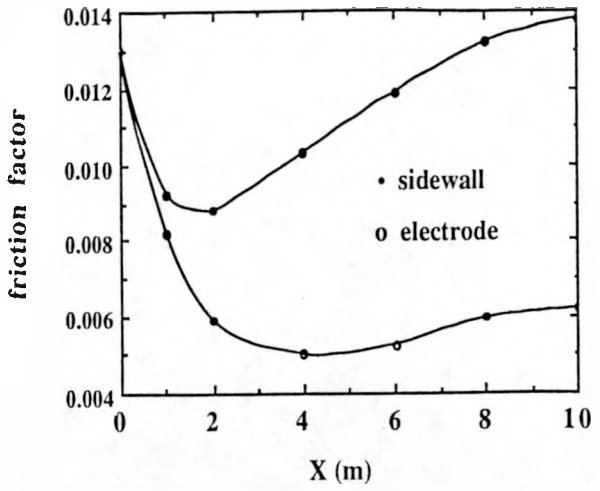

Figure 7. Variation of the friction factor along the duct walls of the MHD generator

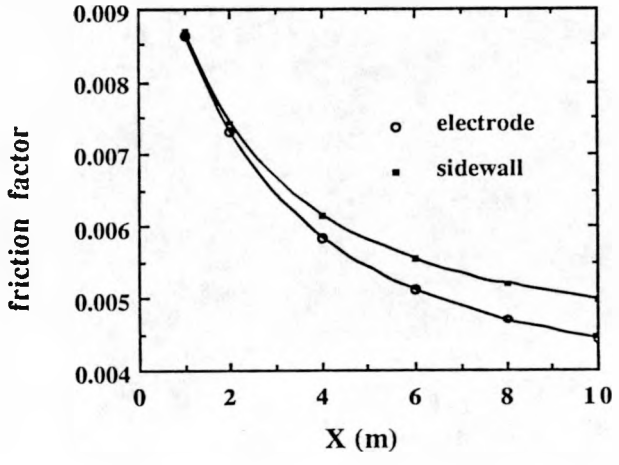

Figure 8. Variation of the factor along the duct walls of the MHD thruster

SUMMARY AND CONCLUSIONS

1. A three-dimensional MHD computer model has been developed and applied to compare the flow characteristics inside MHD plasma generators with those inside seawater thrusters. The governing equations consist of the mass continuity equation, the three momentum equations, the equation for enthalpy (or temperature), turbulence kinetic energy and its dissipation rate and the Maxwell equations.

2. Computations have been performed for a Faraday plasma generator operating with a 6 Tesla magnet and at a load factor K = 0.75, and for an MHD thruster operating in the Faraday mode with continuous electrodes with a 20 Tesla magnet and at a load factor K = 2.0.

3. The three-dimensional effects caused by the interaction of the Lorentz forces (JxB) with the fluid flow are strongly manifested in the case of the MHD generator as compared to the flow development in the thruster. Distinct velocity overshoots exist in the sidewall boundary layers for the case of the generators whereas for the thruster a slightly flatter boundary layer velocity profile exist over the sidewall boundary layer as compared to the velocity profile over the electrode wall.

4. The flow velocity nonuniformities in both applications is caused basically by the nonuniformities of the component of current density J_y in the Hartmann layers of the sidewalls of the MHD ducts. For MHD plasma generators the nonuniform J_y distribution in the Hartmann layers is primarily caused by the strong variation of the electrical conductivity and secondary by the nonuniformity of the velocity in the boundary layers. For MHD seawater thrusters, the electrical conductivity is uniform. Therefore, the nonuniformities of J_y in the sidewall boundary layers are caused primarily by the nonuniformities of the velocity in those layers.

As a result of such velocity nonuniformities, nonuniform distribution of the skin friction exist along the duct walls. The friction coefficient is higher on the sidewalls for both applications but with a distinct difference for the generator case.

REFERENCES

1. Doss, E.D., and Curry, B.P., "Studies of the 3-D Coupled Flows Between the Electrode and Sidewalls of MHD Channels," AIAA paper 76-311, AIAA 9th Fluid and Plasma Dynamics Conference, July 1976.

2. Doss, E.D., and Ahluwalia, R.K., "Three-Dimensional Flow Development In MHD Generators At Part Load," AIAA-82-324, AIAA 20th Aerospace Sciences Meeting, January 1982.

3. Vanka, S.P., Ahluwalia, R.K., and Doss, E.D., "Three-Dimensional Analysis of MHD Generators and Diffusers," Report No. ANL/MHD-87-4, Argonne National Laboratory, 1982.

4. Doss, E.D., Argyropoulos, G.S., and Demetriades, S.T., "Two-Dimensional Flow Inside MHD Ducts with Transverse Asymmetries," AIAA Journal, Vol. 13, No. 5, May 1975, p. 545-546.

5. Doss, E., Geyer, H., Ahluwalia, R.K., and Im, K., "Two-Dimensional Performance Analysis and Design of MHD Channels," J. Fluids Engineering, Vol. 103, June 1981, pp 307-314

6. Ahluwalia, R.K., and Doss, E.D., "Quasi-Three Dimensional Modeling of Flow in MHD Channels," Numerical Heat Transfer, Vol. 3, 1980, p. 67-87.

7. Roy, G.D., and Wu, Y.C.L., "Study of Pressure Distribution Along Supersonic MHD Generator Channel," AIAA J., Vol. 13, No. 9, September 1975.

8. Ahluwalia, R.K., and Doss, E.D., "Convective Heat Transfer in MHD Channels and Its Influence on Channel Performance," J. Energy, Vol. 4, No. 3, May-June 1980, pp. 126-134.

9. Phillips, O. M., "The Prospects for Magnetohydrodynamic Ship Propulsion," J. Ship Research, Vol 43, March 1962, pp. 43-51.

10. Doragh, R.A., "Magnetohydrodynamic Ship Propulsion Using Superconducting Magnets," Proc. Naval Arch. and Marine Engineers Transaction, Vol. 71, 1963.

11. Way, S., "Electromagnetic Propulsion for Cargo Submarines," Journal of Hydraulics, Vol. 2, No. 2, April 1968, pp. 49-57.

12. Saji, Y., Kitano, M., and Iwata, A., "Basic Study of Superconducting Electromagnetic Thrust Device for Propulsion in Sea Water," Advances in Cryogenic Engineering (Timmerhans, K.D. editor), Vol. 23, 1978, pp. 159-169.

13. Hummert, G.T., "An Evaluation of Direct Current Electromagnetic Propulsion In Seawater," Report ONR-CR168-007-1, Westinghouse Research Laboratories, Pittsburgh, Pennsylvania, July 1979.

14. Cott, D.W., et al, "MHD Propulsion For Submarines," CDIF External Report No. 2 DOE-MHD-D140, MSE Inc., Butte, Montana, October 1988.

15. Vanka, S.P. and Ahluwalia, R.K., "Coupled Three-Dimensional Flow and Electrical Calculations for Faraday MHD Generators," Paper No. AIAA-81-1230, AIAA 14th Fluid and Plasma Dynamics Conference, Palo Alto, CA, June 1981.

16. "McGraw-Hill Encyclopedia of Science and Technology," 6th Edition, Vol. 16, pp. 144-178, McGraw-Hill Book Company, New York, 1987.

17. Doss, E.D., and Roy, G., "Effects of Strong Magnetic Fields On Flow Characteristics of MHD Seawater Propulsion System," 10th International Conference on MHD Electrical Power Generation, December 4-8, 1989, India.

ACKNOWLEDGEMENT

This work has been sponsored by the Office of Naval Research, U.S., under Contract No. N00014-89-F-0064.